










## Article

# Metabolomic Insights into the Potential of Chestnut Biochar as a Functional Feed Ingredient

Serena Reggi <sup>1,\*</sup> , Sara Frazzini <sup>1</sup> , Simone Pedrazzi <sup>2</sup> , Martina Ghidoli <sup>3</sup> , Maria Claudia Torresani <sup>4</sup>, Marco Puglia <sup>2</sup> , Nicolò Morselli <sup>2</sup>, Marianna Guagliano <sup>5</sup>, Cinzia Cristiani <sup>5</sup> , Salvatore Roberto Pilu <sup>3</sup> , Elisabetta Onelli <sup>6</sup> , Alessandra Moscatelli <sup>6</sup> and Luciana Rossi <sup>1</sup> 

<sup>1</sup> Department of Veterinary Medicine and Animal Sciences—DIVAS, University of Milano, Via dell'Università 6, 26900 Lodi, Italy; sara.frazzini@unimi.it (S.F.); luciana.rossi@unimi.it (L.R.)

<sup>2</sup> Department of Engineering-Enzo Ferrari, University of Modena and Reggio Emilia, Via Università 4, 41121 Modena, Italy; simone.pedrazzi@unimore.it (S.P.); marco.puglia@unimore.it (M.P.); nicolo.morselli@unimore.it (N.M.)

<sup>3</sup> Department of Agricultural and Environmental Sciences-Production Landscape and Agroenergy, University of Milano, Via Celoria 2, 20133 Milano, Italy; martina.ghidoli@unimi.it (M.G.); salvatore.pilu@unimi.it (S.R.P.)

<sup>4</sup> Biotecnologie BT srl., Parco Tecnologico Padano (PTP), Via Albert Einstein, 26900 Lodi, Italy; ctorresani@biotecnologiebt.it

<sup>5</sup> Department of Chemistry, Materials and Chemical Engineering—Giulio Natta, Politecnico of Milan, Piazza Leonardo Da Vinci, 32, 20133 Milano, Italy; marianna.guagliano@polimi.it (M.G.); cinzia.cristiani@polimi.it (C.C.)

<sup>6</sup> Department of Biosciences, University of Milan, Via Celoria 26, 20133 Milano, Italy; elisabetta.onelli@unimi.it (E.O.); alessandra.moscatelli@unimi.it (A.M.)

\* Correspondence: serena.reggi@unimi.it

**Abstract:** Biochar is potentially a functional ingredient in animal nutrition that offers health benefits such as detoxification, while also promoting environmental sustainability through carbon sequestration, emission reduction, and its circular production. However, the heterogeneity of commercially available biochar products requires a detailed assessment of their functional properties for applications in animal feed. This study evaluates chestnut biochar from morphological, chemical, and metabolomic perspectives and assesses its functional properties. Metabolomic analysis of a water extract using QTOF HPLC-MS/MS confirmed the presence of bioactive compounds, such as hydroxybenzoic and succinic acids, highlighting its potential as a functional feed ingredient. The chestnut biochar inhibited the growth of the pathogenic *E. coli* strains F18+ and F4+, with maximum inhibition rates of 15.8% and 28.6%, respectively, after three hours of incubation. The downregulation of genes associated with quorum sensing (MotA, FliA, FtsE, and HflX, involved in biofilm formation and cellular division) suggests that biochar interferes with several aspects of the pathogenic process. Importantly, biochar was not found to adversely affect beneficial probiotic bacteria, such as *Lactiplantibacillus plantarum* and *Limosilactobacillus reuteri*. These findings support the potential of chestnut biochar as a versatile ingredient for sustainable animal nutrition, thus promoting animal welfare while offering environmental benefits.

**Keywords:** biochar; waste and by-product; circular economy; chestnut; functional properties; feed



Academic Editors: Seong-Jik Park and Mónica Calero de Hoces

Received: 24 October 2024  
Revised: 24 December 2024  
Accepted: 16 January 2025  
Published: 22 January 2025

**Citation:** Reggi, S.; Frazzini, S.; Pedrazzi, S.; Ghidoli, M.; Torresani, M.C.; Puglia, M.; Morselli, N.; Guagliano, M.; Cristiani, C.; Pilu, S.R.; et al. Metabolomic Insights into the Potential of Chestnut Biochar as a Functional Feed Ingredient. *Appl. Sci.* **2025**, *15*, 1084. <https://doi.org/10.3390/app15031084>

**Copyright:** © 2025 by the authors. Licensee MDPI, Basel, Switzerland. This article is an open access article distributed under the terms and conditions of the Creative Commons Attribution (CC BY) license (<https://creativecommons.org/licenses/by/4.0/>).

## 1. Introduction

Biochar, a carbon-rich material produced through the thermal degradation of biomass via pyrolysis or gasification at temperatures above 350 °C without or with limited oxygen, has gained increasing attention due to its potential application in environmental management, including carbon sequestration and soil health improvement [1]. Biochar was listed

as vegetable charcoal in the European feed material catalog in 2011 (Reg EU 2022/1104). More recently, its use in animal nutrition has gained increased attention due to its benefits for animal health and its contribution to sustainability in line with agroecological principles [2,3].

The incorporation of biochar into animal feed promotes health and well-being in different species and also helps combat antibiotic resistance [4,5]. Biochar also binds toxins of various origins, reduces greenhouse gas emissions, and functions as a circular product through recycling [6,7]. These properties highlight its potential as a multifaceted tool for advancing both animal health and environmental sustainability.

The distinctive characteristics of biochar, including its chemical composition (nutrient content, ash content, and pH), physical structure (porosity, surface area, and particle size), and overall efficiency (adsorption and cation exchange capacity) can vary significantly depending on the type of biomass used and the production process [8,9]. These variations influence the effectiveness of biochar in different applications, thus emphasizing the need for careful selection and optimization of both feedstock and pyrolysis conditions to achieve the desired use [10,11].

Chestnut wood (*Castanea sativa*) works particularly well in biochar production, especially in terms of its agro-residues. Chestnut trees are cultivated in a vast geographical range and thus provide a readily available feedstock, and the lignocellulosic component of chestnuts optimizes pyrolysis [12]. The gasification of chestnut-based biomasses is considered an efficient and sustainable agricultural process, boosting bio-energy production and the recycling of by-products.

Exploiting chestnut biochar could regenerate abandoned chestnut orchards in many areas across Europe and improve the landscape. This aligns with the objectives of the 2030 Agenda for Sustainable Development, which emphasizes the need for sustainable land management and environmental restoration.

The agro-residues from chestnut processing, including the pericarp (8.9–13.5%) and integument (inner shell, 6.3–10.1%), generate significant waste. Despite the challenges associated with their disposal, these by-products are valuable sources of bioactive molecules and can be transformed into high-value products. Chestnut wood, along with the pericarp and integument, contains significant amounts of phenolic compounds, such as hydrolyzable tannins, flavonoids, and phenolic acids (e.g., gallic acid and ellagic acid), which possess antioxidant properties and are already used in animal nutrition [13].

These compounds may persist in the biochar derived from chestnut, potentially increasing its benefits for animal health and integrating the natural properties of biochar. Functional nutrition improves animal health, performance, and sustainability, thus reducing the use of antibiotics. It also aligns with both economic and ethical considerations in animal management.

Given the significant variations in the properties of biochar based on feedstock and production conditions, our aim was to characterize each type thoroughly to optimize its applications in animal nutrition, especially given that the literature on chestnut biochar in animal nutrition is both limited and inconsistent.

This study characterizes the chestnut agro-residue biochar (CB) in terms of its chemical composition, morphological features, and functional properties. The aim is to provide a comprehensive understanding of the potential benefits and effectiveness of chestnut biochar, particularly in terms of animal nutrition and environmental sustainability.

## 2. Materials and Methods

### 2.1. Production of Chestnut Agro-Residue Biochar

Chestnut agro-residue biochar (CB) was produced using the “Femto Gasifier”, a lab-scale gasification prototype with a single throat downdraft architecture. In this system, biomass undergoes four main phases: drying ( $>100\text{ }^{\circ}\text{C}$ ), pyrolysis ( $500\text{--}700\text{ }^{\circ}\text{C}$ ), combustion ( $\approx 1000\text{ }^{\circ}\text{C}$ ), and reduction ( $\approx 800\text{ }^{\circ}\text{C}$ ) [14] (Figure 1). Pyrolysis is a sequence of endothermic and exothermic reactions that degrade biomass by heating it in the absence of oxygen. During this process, biomass decomposes, forming char, gases ( $\text{CO}$ ,  $\text{CO}_2$ , and  $\text{CH}_4$ ), condensable vapors containing organic compounds, and water [14]. During combustion, a fraction of the carbon and hydrogen present in the biomass is oxidized, releasing a large amount of heat that sustains the endothermic processes [15]. Below the combustion zone, reduction reactions occur. The main are the water-gas reaction ( $\text{C} + \text{H}_2\text{O} \leftrightarrow \text{CO} + \text{H}_2 - 131.4\text{ kJ/gmol}$ ), bounded reaction ( $\text{C} + \text{CO}_2 \leftrightarrow 2\text{CO} - 172.6\text{ kJ/gmol}$ ), shift reaction ( $\text{CO}_2 + \text{H}_2 \leftrightarrow \text{CO} + \text{H}_2\text{O} - 42\text{ kJ/gmol}$ ), and methane reaction ( $\text{C} + 2\text{H}_2 \leftrightarrow \text{CH}_4 + 75\text{ kJ/gmol}$ ). As the char descends through the reduction zone, its degree of burn-off increases. Due to char-gas reactions and particle shrinkage, the char size decreases while its porosity increases [16].

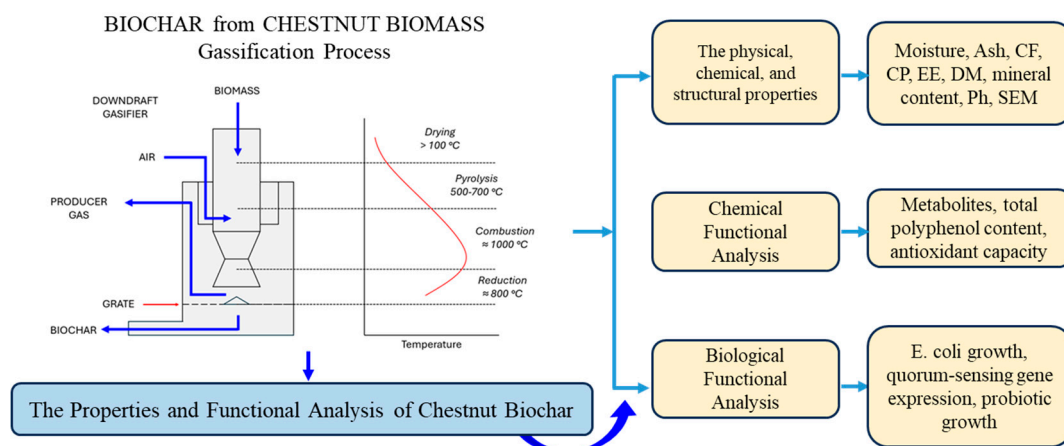


**Figure 1.** The chestnut biochar production process and flow chart of the study.

The gasifier was initially started using small woodchips from shredded *Prunus* branches. Once the system had reached the designated operating temperature, chestnut shells were introduced as feedstock, replacing the woodchips. Air, used as the gasification medium, was supplied by a side channel blower, and the producer gas was combusted in a flare. CB that passed through the grate at the bottom of the reactor was conveyed via an extraction auger in a collection vessel. All the CB used in the present study was collected from the vessel the day after the gasification test, allowing the system to cool to ambient temperature. The CB produced was derived from approximately 70% woodchips and 30% chestnut shells, obtained from a single material collection in the Piedmont region (Italy).

### 2.2. Evaluation of Chemical Characteristics and Composition of Chestnut Agro-Residue Biochar

A total of 15 g of CB was analyzed to determine the moisture content, ash content, crude fiber (CF), crude protein (CP), and ether extract (EE). The chemical analyses were conducted in accordance with the “Official Methods of Analysis” of AOAC International (22nd edition, 2023) [17]. In brief, dry matter (DM) was determined by drying samples in a forced-air oven at  $65\text{ }^{\circ}\text{C}$  for 24 h (AOAC method 930.15). Ash content was measured by incinerating the samples in a muffle furnace at  $550\text{ }^{\circ}\text{C}$  for three hours (method 942.05). CF was analyzed using the filter bag method (AOCS method Ba 6a-05). The CP content was determined by the Kjeldahl method (AOAC method 2001.11), and the EE was quantified

using ether extraction with a Soxhlet apparatus (DM 21/12/1998). All analyses were performed in triplicate.

### 2.3. Evaluation of the Mineral Content of Chestnut Agro-Residue Biochar

Samples of chestnut agro-residue biochar (0.3 g DM each) were mineralized using the MULTIWAVE 3000 Microwave Digestion System (Anton Paar GmbH, Graz, Austria) in a single reaction chamber. The samples were placed in Teflon tubes and treated with 10 mL of concentrated HNO<sub>3</sub> (65%). The temperature was ramped to 120 °C over a period of 10 min and then maintained at 120 °C for an additional 10 min. After mineralization, the samples were cooled for 20 min and transferred to polypropylene test tubes. The mineralized samples were diluted 1:100 with a standard solution containing an internal standard (100 µL) and 10 mL of 0.3 M HNO<sub>3</sub> in Milli-Q water. Elemental concentrations were determined using an ICP-MS (BRUKER Aurora-M90 ICP-MS, Bremen Germany). The mineral composition of the samples was assessed using calibration curves for the following elements: Na, Mg, Al, K, Ca, Cr, Mn, Fe, Co, Ni, Cu, Zn, As, Se, Mo, Cd, Pb, and P. To check the nebulization performance, an aliquot of 2 mg/L of a standard solution (72Ge, 89Y, 159Tb) was added to the samples until a final concentration of 20 µg/L was achieved. To reduce polyatomic interferences, a collision-reaction interface (CRI) was used with an H<sub>2</sub> flow rate of 80 mL/min through the skimmer cone.

### 2.4. Scanning Electron Microscopy

For observations using scanning electron microscopy (SEM), CB samples were directly placed on the stub and sputtered with carbon. Observations were performed under an FE-SEM Sigma (Zeiss, Oberkochen, Germany) at 8 KV and a working distance of 5 mm. The size of the samples and porous were measured using ImageJ (Version: 1.54). The values were processed for statistical analysis (*t*-test) by Microsoft Excel (Microsoft Office 16).

### 2.5. Preparation of Water Extracts from the Chestnut Agro-Residue Biochar

The CB extracts were prepared using an eco-friendly green chemistry method according to Lou et al. [18], with minor modifications. Briefly, 30 g of CB was manually homogenized using a mortar and pestle. Then, 10 g of homogenized CB was suspended in 200 mL of demineralized water and heated in a water bath at 90 °C for 4 h. Subsequently, the mixture was subjected to rotary shaking at 180 rpm at room temperature (25 °C) for 24 h. The solid phase of CB was separated from the liquid phase by centrifugation at 4 °C for 20 min. To ensure thorough separation, the supernatant was filtered again using a 0.22 µm syringe filter. The liquid extracts were then stored at −20 °C until analysis. The pH was measured using a pH meter (Thermo Fisher Scientific, Waltham, MA, USA).

### 2.6. QTOF HPLC MS/MS Metabolomic Characterization of the Chestnut Agro-Residue Biochar Extract

Qualitative metabolomic analysis of CB extracts was performed using Q-TOF HPLC MS/MS (Sciex, Framingham, MA, USA). The separation column used was a Synergy Hydro- RP 80Å, LC column 250 mm, 4.6 mm, 4 µm (Phenomenex, LaneCove, Australia) set at a temperature of 25 °C with a binary mobile phase: A (H<sub>2</sub>O with 1% formic acid) and B (acetonitrile with 0.1% of formic acid). The gradient elution program was a 0.4 mL min<sup>−1</sup> flow rate with a linear gradient: from 0 to 5 min 0.5% of A and 95.5% of B; from 5 to 25 min 75% of A and 25% of B; from 25 to 31 min 5% of A and 95% of B; and from 31 to 35 min 95% of A and 5% of B. The injection volume was 10 µL. MS/MS analysis was performed in both positive and negative modes. The raw data were analyzed using two libraries, metabolites, and natural compounds (Sciex OS version 3.1, Framingham, MA, USA)

### 2.7. Evaluation of the Total Polyphenol Content of the Chestnut Agro-Residue Biochar Extract

The total polyphenol content (TPC) of the CB extract was evaluated by the Folin-Ciocalteu colorimetric method, according to Perez et al. [19]. Specifically, 2 mL of Folin-Ciocalteu (FC) reagent was added to 2 mL of CB extract. After 3 min, 750  $\mu$ L of anhydrous sodium carbonate solution (7.5%, *w/v*) was added and the mixture was diluted to 10 mL with distilled water. After one hour, the absorbance was recorded at 765 nm. Calibration curves were constructed using tannic acid as the standard at concentrations ranging from 0 to 240  $\mu$ g/mL. Each sample and calibration point were measured in triplicate. The TPC was expressed as tannic acid equivalent (TAE) in  $\mu$ g/gr biochar.

### 2.8. Evaluation of the Antioxidant Capacity of the Chestnut Agro-Residue Biochar Extract

The antioxidant capacity (AOX) of the CB extract was determined according to Ilyasov et al. [20]. A Trolox stock solution (2.5 mM in distilled water) was used to construct the standard curve. A solution of 2,2'-azinobis (3-ethylbenzothiazolin-6-sulphonic acid (ABTS) (7 mM) was prepared by reacting it with 140 mM potassium persulphate in distilled water and allowing the mixture to stand in the dark for 12 h to produce the ABTS $\bullet$ + solution. For the AOX capacity assay, the ABTS $\bullet$ + solution was diluted with phosphate-buffered saline, pH 7.4 (PBS) to obtain an absorbance of  $0.706 \pm 0.01$  at 734 nm. Then, 10  $\mu$ L of CB extract or Trolox standard was mixed with 1 mL of ABTS $\bullet$ + solution and incubated in the dark at room temperature for 15 min before reading the absorbance at 734 nm using a spectrophotometer (UV/VIS Lambda 365, PerkinElmer, Waltham, MA, USA). The percentage inhibition of the absorbance at 734 nm was calculated and plotted against the concentration of the Trolox standard curve. AOX results were expressed as  $\mu$ mol Trolox equivalents (TE) per gram of extract.

### 2.9. Evaluation of the Chestnut Agro-Residue Biochar Extract on *E. coli* Growth

The effect was assessed of the CB extract on the growth of two fimbriated *E. coli* strains, F4 (F4+) and F18 (F18+), which have adhesive fimbriae. These strains were obtained from the collection of the Department of Veterinary Medicine and Animal Science, University of Milan (Italy). Overnight cultures (200  $\mu$ L) of *E. coli* were inoculated into tubes containing 15 mL of Luria-Bertani (LB) medium, supplemented with 0, 25, 50, and 100  $\mu$ L/mL of CB extract. Prior to inoculation, bacterial densities were normalized using spectrophotometry (UV/VIS Lambda 365, PerkinElmer, Waltham, MA, USA) at 600 nm ( $OD_{600} = 0.03$ ). The tubes were incubated aerobically at 37 °C with shaking at 180 rpm. Bacterial growth was monitored by measuring the optical density at 600 nm ( $OD_{600}$ ) at 60-min intervals using a spectrophotometer (UV/VIS Lambda 365, PerkinElmer, Waltham, MA, USA). Bacteria-free tubes containing equivalent concentrations of biochar extract served as blanks. Optical density data were converted to cell counts (CFU/mL) using a calibration curve. The analysis was performed in biological duplicates with three technical replicates each.

### 2.10. Quorum Sensing Gene Expression in *E. coli* Treated with CB Extract

Overnight bacterial cultures of *E. coli* F4+ and F18+ were diluted in a sterile LB medium to reach an optical density of 0.03 at 600 nm. Subsequently, 15 mL of each bacterial suspension was incubated with the CB extract (100  $\mu$ L/mL) for 3 h at 37 °C. The total RNA was extracted from each bacterial culture incubated with the CB extract using the RNA Basic Kit FastGene (Nippon Genetics Europe, Düren, Germany). The concentration and optical absorbance of each extracted RNA were confirmed with a NanoDrop spectrophotometer (Thermo Fisher Scientific, MA, USA) at 260 nm/280 nm.

RNA samples were stored at  $-80$  °C. The cDNA was synthesized using the iScript cDNA Synthesis Kit (Bio-Rad, Hercules, CA, USA) following the manufacturer's instruc-

tions. RT-PCR was performed for cDNA synthesis confirmation. Quantitative Real-Time PCR was performed by the ss Advanced Universal SYBR Green Mix (Bio-Rad, CA, USA) gene expression assay. The primers used are listed in Table 1.

Relative expression was calculated by the  $2^{-\Delta\Delta CT}$  method, using the GapA gene as the housekeeping gene [21]. In addition to melting curve analysis, the specificity of each primer was confirmed by DNA sequencing of the Real-Time PCR product. The melting curve analysis was performed over a temperature range of 65–95 °C, with 0.5 °C increments every 5 s. The thermal program consisted of an initial denaturation at 95 °C for 5 min, followed by 40 cycles of 95 °C for 15 s and 60 °C for 30 s. Each experiment was performed in triplicate.

**Table 1.** List of primers used for qRT PCR.

Target	Nucleotide Sequence	Acc. N°	Size	Ref.
GapA	FW-GAAATGGGACGAAGTTGGTG Rv-AACCACTTTCTTCGCACCAG	NP_416293	104 bp	[22]
FliA	FW-GCTGGCTGTTATTGGTGTCG Rv-CAACTGGAGCAGGAACTTGG	NP_416432	112 bp	[22]
MotA	FW-CTTCCTCGGTTGTCGTCTGT Rv-CTATCGCCGTTGAGTTTGGT	NP_416404	120 bp	[22]
FtsE	FW-AAAGTACCCTCCTGAAGCTGATCTGTG Rv-GCGTGATGTCATGGCCGCTAAAC	NP_417920	81 bp	[22]
HflX	FW-TGTAGGTGAAGGTAAAGCAG Rv-CACGACACTCGCACAAACGC	NP_418594	128 bp	[22]

### 2.11. Effects of Chestnut Agro-Residue Biochar Extract on Probiotic Strains

The CB extract was also tested for its effect on the growth of probiotic strains, specifically *Lactiplantibacillus plantarum* and *Limosilactobacillus reuteri* that had already been characterized by our research group both in vitro and in vivo [23,24]. Bacteria were grown in a broth at 30 °C without shaking for 12 h, and these cultures were used as inoculants for all the experiments. Overnight cultures (500 µL) of *L. plantarum* and *L. reuteri*, respectively, were inoculated into tubes containing 15 mL of Man Rogosa Sharpe (MRS) medium (optical density of 0.12 at 600 nm) and supplemented with 0, 50, and 100 µL/mL of the CB extract. The cultures were statically incubated at 30 °C, and bacterial growth was monitored by measuring the optical density at 600 nm (OD<sub>600</sub>) at 120-min intervals using a spectrophotometer (UV/VIS Lambda 365, PerkinElmer, Waltham, MA, USA). Bacteria-free tubes containing MRS medium and equivalent concentrations of biochar extract were used as negative controls. The analysis was conducted in biological duplicate, with three technical replicates each.

### 2.12. Statistical Analysis

All data are shown as mean ± standard deviation ( $n = 3$ ). Statistical analyses were performed by GraphPad Prism (version 9.0.0, 2020), and the two-way ANOVA was used in order to compare time, treatments, and their interaction. The symbol \* indicates a significant difference  $p \leq 0.05$ , and \*\* indicates a significant difference  $p \leq 0.001$ .

## 3. Results

### 3.1. Chemical Composition and Mineral Content of the Chestnut Agro-Residue Biochar

The char yield was approximately 5% of the initial biomass mass (on a dry matter basis). Based on an average feedstock bulk density of 300 kg/m<sup>3</sup> and a biochar bulk density of

500 kg/m<sup>3</sup>, biochar production was estimated to be 0.03 m<sup>3</sup> for every m<sup>3</sup> of biomass. The CB obtained was found to have an ash content of 25 ± 0.25%, dry matter (DM) of 91.51 ± 0.12%, crude protein (CP) ≤ 1%, an undetectable ether extract (EE), and a fiber content of 9.01 ± 2.68%. The biochar was characterized by high levels of mineral components, including alkali metals (K and Na) and alkaline earth metals (Ca and Mg) (Table 2). In addition, the concentrations of contaminant heavy metals (As, Pb, and Cd) were below the maximum permitted levels in feed (Dir. 2002/32/UE and Reg. UE N. 744/2012).

**Table 2.** Mineral content of CB biochar by ICP-MS. The results are expressed as the mean ± sd (*n* = 3).

Mineral	Content (g kg <sup>-1</sup> )	Mineral	Content (mg kg <sup>-1</sup> )	Mineral	Content (mg kg <sup>-1</sup> )
Na	10.34 ± 1.70	Cr	66.56 ± 8.22	Zn	1477.47 ± 321.71
Mg	7.36 ± 1.16	Mn	721.99 ± 170	As	2.06 ± 0.41
Al	2.74 ± 0.11	Fe	6720 ± 0.61	Se	0.15 ± 0.05
P	3.34 ± 0.62	Co	1.93 ± 0.51	Mo	2.38 ± 1.59
K	33.56 ± 3.06	Ni	28.72 ± 6.66	Cd	0.20 ± 0.04
Ca	9.31 ± 1.09	Cu	59.89 ± 1.50	Pb	8.05 ± 0.39

### 3.2. Morphological Characterization

The morphology of the biochar was examined by SEM. At low magnification (Figure 2A), a mixture of small and large fragments was observed. However, the overall texture of the sample consisted mostly of fragments with dimensions of approximately 100–300 µm (considering the largest fragment coordinates). Only a few materials had dimensions of 1 mm or as small as 50 µm. Many of these fragments had retained the structural characteristics of the original plant tissues. Many aggregations of vascular and fibrous cells (Figure 2B–E) were found, probably derived from chestnut wood or vascular bundles of fruit remains. The lignin in the cell wall led to good preservation of these structures.

The tracheids were well structured (Figure 2B,C), with smooth cell walls, characterized by oval pits (taxodioid; Figure 2C, arrows). The shape and organization of these pits confirmed that they belonged to chestnut wood [25]. Fibers appeared as closely packed cells with a regular diameter (Figure 2D,E), sometimes flattened by treatment (Figure 2D, asterisk), with smooth cell walls. Occasionally, debris, probably derived from the breakage of cells from living tissue (parenchymal cells), filled the cell cavities of these fibers, blocking their lumen (Figure 2E, arrows). The average lumen area of these cells was 27 µm<sup>2</sup>, while the average lumen area of the thinner end of the tapered cells was 1.5 µm<sup>2</sup>.

In addition to lignified cells, other different tissues were recognizable in the fragments. The integumentary tissues showed neighboring cells with no intercellular space (Figure 2F). Some fractures were visible along the middle lamella (Figure 2F, arrow) and the proximal cell wall of some cells had disappeared (Figure 2F, asterisk), probably due to the sample preparation. Parenchymal tissues were characterized by large cells with a main dimension of 50 µm and an area of one mm<sup>2</sup> (Figure 2G, asterisk). The fragment in Figure 2G shows parenchymal cells surrounding a fiber aggregate (Figure 2G, arrow). The cells on the surface of the fragment lacked the proximal cell wall and contained cell debris (Figure 2G). Debris lost during cell treatment had aggregated to form fragments of amorphous material in which plant tissue was not observed (Figure 2D, arrows).

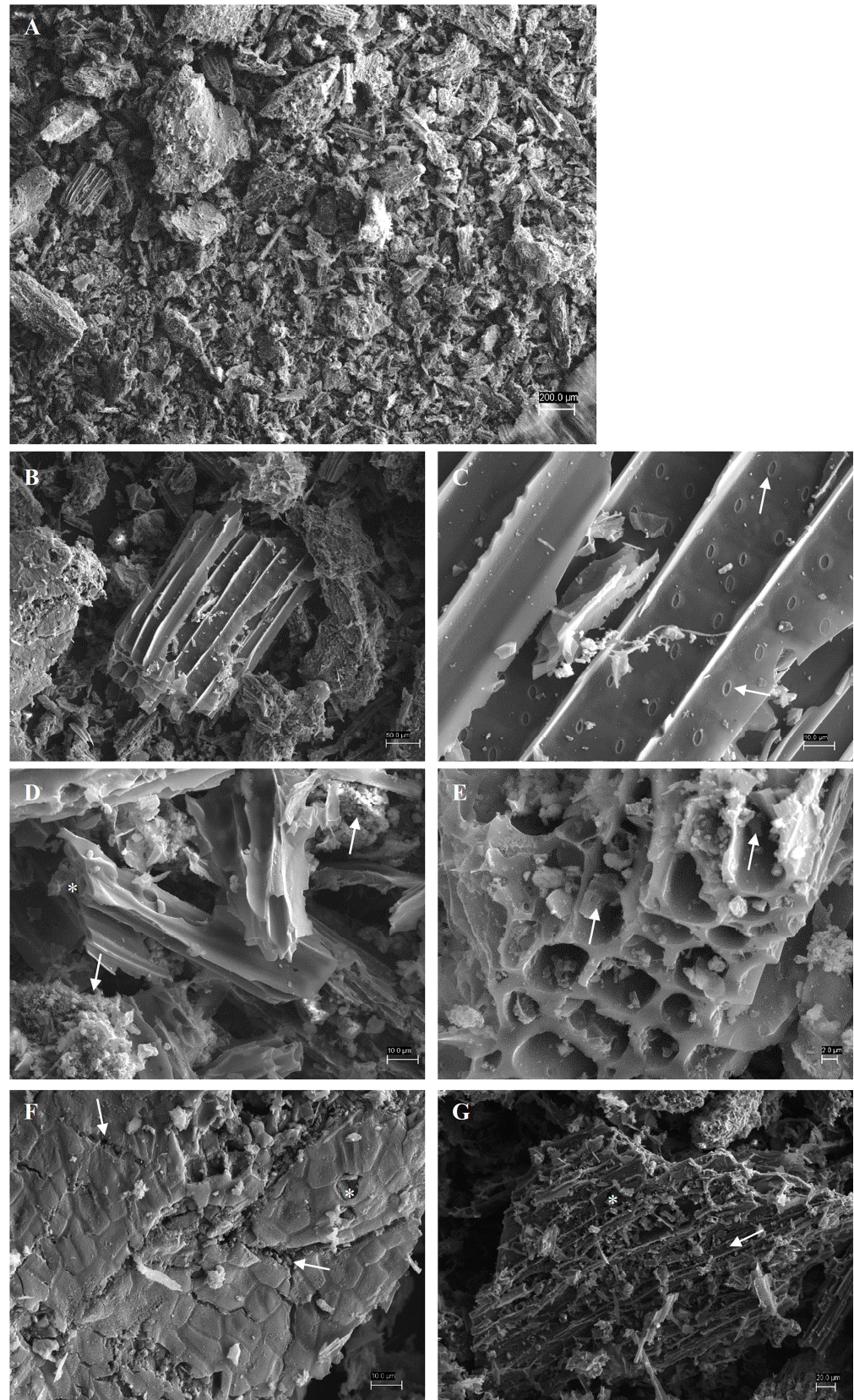


**Figure 2.** Morphological analysis of biochar from chestnut agro-residue biomass by scanning electron microscope (SEM). (A) Image at low magnification; (B–G) Image at high magnification.



### 3.3. Chemical and Metabolomic Characterization of Chestnut Agro-Residue Biochar Extract

The data obtained showed that the pH of the chestnut biochar (CB) extract was alkaline, measuring  $10.15 \pm 0.43$ . Metabolomic analysis of the CB extract conducted by QTOF HPLC MS-MS revealed bioactive molecules (Table 3). The extract was predominantly composed of simple aromatic compounds and small polyphenols with four to seven carbon atoms. Notably, isomers of hydroxybenzoic acid were identified, including m-hydroxybenzoic acid, which showed a hydroxyl group positioned at the meta position relative to the carboxyl group on the benzene ring.

**Table 3.** Metabolomic profile of CB extract.

Component	Formula	Area	Retention Time	Adduct
4-Hydroxybenzoic acid	C <sub>7</sub> H <sub>6</sub> O <sub>3</sub>	108,484	8.35	[M-H] <sup>-</sup>
Azelaic acid	C <sub>9</sub> H <sub>16</sub> O <sub>4</sub>	1,830,729	8.02	[M-H] <sup>-</sup>
Succinic acid	C <sub>4</sub> H <sub>6</sub> O <sub>4</sub>	365,375	1.67	[M-H] <sup>-</sup>
6-Methylcoumarin	C <sub>10</sub> H <sub>8</sub> O <sub>2</sub>	20,094	8.15	[M-H] <sup>+</sup>
7-Methoxycoumarin	C <sub>10</sub> H <sub>8</sub> O <sub>3</sub>	118,168	7.97	[M-H] <sup>+</sup>
7-Hydroxycoumarin	C <sub>9</sub> H <sub>6</sub> O <sub>3</sub>	337,625	6.98	[M-H] <sup>+</sup>

### 3.4. Evaluation of the Total Polyphenol Content and Antioxidant Capacity of Chestnut Agro-Residue Biochar Extract

The CB extract showed a total polyphenol content of  $149.22 \pm 4.02$  µg/g and exhibited an antioxidant (AOX) activity of  $91.5 \pm 0.84$  µg/mL of Trolox equivalents (TE).

### 3.5. Effects of Chestnut Agro-Residue Biochar Extract on *E. coli* Growth

The growth of *E. coli* strains F4+ and F18+ was tested in the presence of different concentrations (0, 25, 50, and 100 µL/mL) of CB extract, which inhibited *E. coli* growth. Both strains entered the logarithmic phase after one hour, with inhibitory activity observed after 2 h, which persisted for up to 4 h. Pathotype F4+ was more sensitive than F18+. The maximum inhibition rates at the highest concentration (100 µL/mL) were 28.6% for F4+ and 15.8% for F18+ after 3 h of incubation with the CB extract (Figure 3).

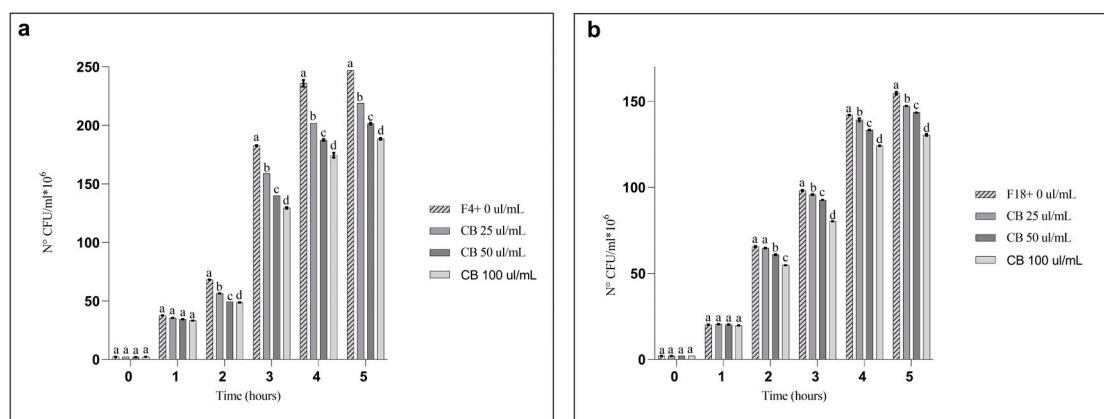


**Figure 3.** Growth inhibition of CB extract against *E. coli*. (a) Growth inhibition of *E. coli* F4+. (b) Growth inhibition of *E. coli* F18+. Data are shown as the means and standard deviations. Different superscript letters indicate significant differences at  $p < 0.05$  among different concentrations within the same time point.

### 3.6. Quorum Sensing Gene Expression in *E. coli* Treated with Chestnut Agro-Residue Biochar Extract

The results on quorum sensing gene expression in *E. coli* indicate that the chestnut agro-residue biochar extract effectively downregulated key quorum sensing genes, with a more pronounced effect in the F4+ strain compared to F18+. Specifically, the relative expression of FliA, MotA, FtsE, and HflX genes in *E. coli* F4+ showed significant downregulation. In contrast, while FliA, MotA, and FtsE were downregulated in *E. coli* F18+, no significant differences were observed for HflX (Figure 4).

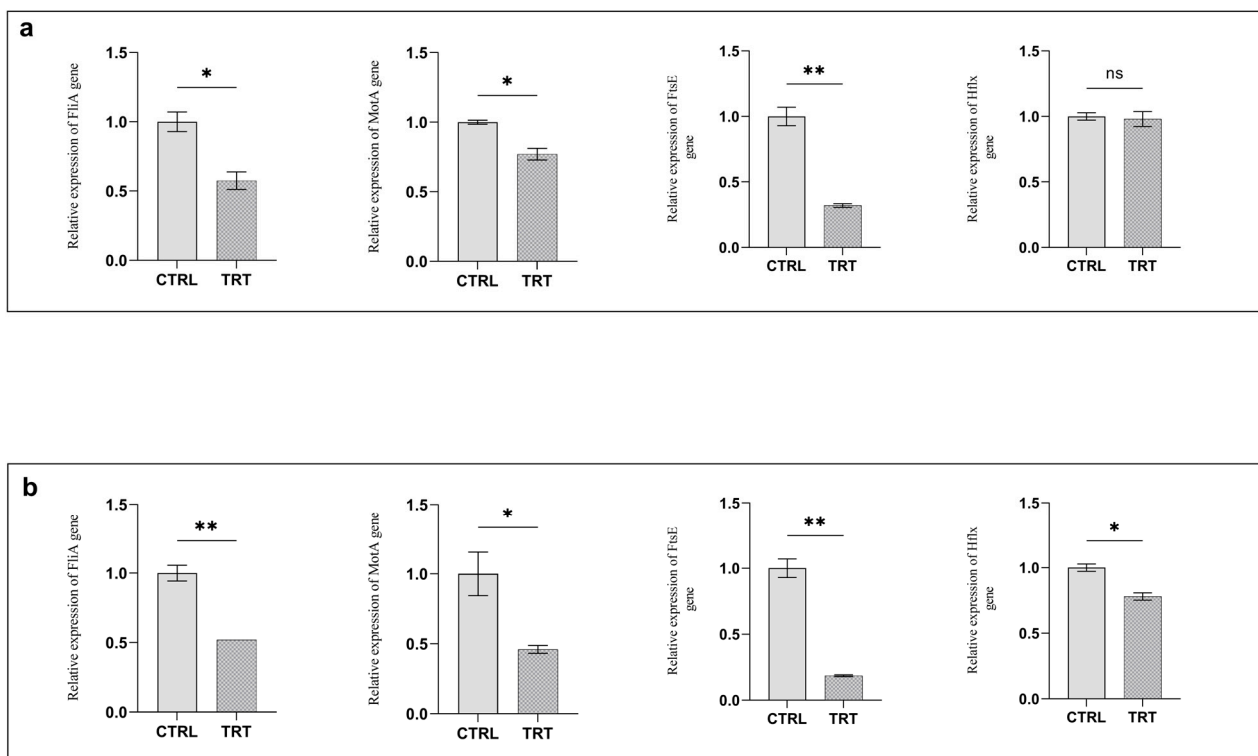


**Figure 4.** Relative expression of the FliA, MotA, FtsE, and Hflx genes. (a) Relative expression of *E. coli* F4+ at 3 h of coculture with 100  $\mu\text{L}/\text{mL}$  di CB extract; (b) Relative expression of *E. coli* F18+ at 3 h of coculture with 100  $\mu\text{L}/\text{mL}$  di CB extract. The symbol \* indicates a significant difference  $p \leq 0.05$ , and \*\* indicates a significant difference  $p \leq 0.001$ , ns indicates not significant.

### 3.7. Effects of Chestnut Agro-Residue Biochar Extract on Probiotic Strains

Evaluation of the effects of the CB extract on probiotic strains showed that both *L. plantarum* and *L. reuteri* were unaffected by concentrations of 50 and 100  $\mu\text{L}/\text{mL}$  of CB extract, thus indicating that the CB extract has no toxic effects. As shown in Figure 5, the growth curve of *L. reuteri* with the CB extract was comparable to that of the control. Notably, *L. plantarum* exhibited a significant increase ( $p \leq 0.05$ ) in growth from 4 to 6 h of incubation with the CB extract.

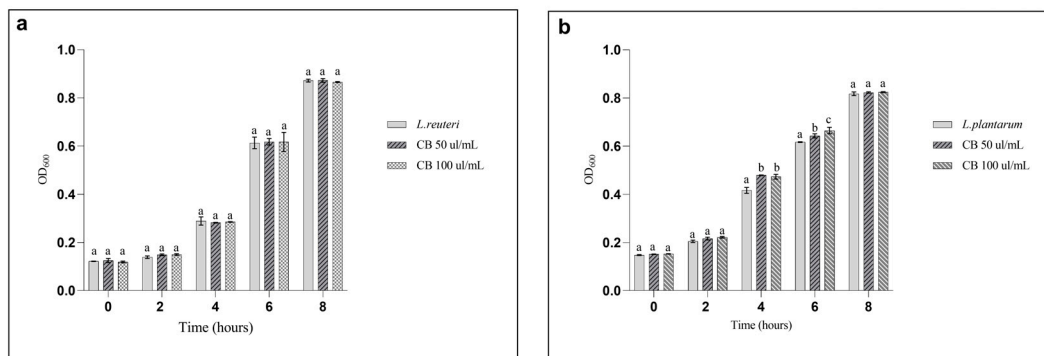


**Figure 5.** (a) *L. reuteri* growth with 0, 50, and 100  $\mu\text{L}/\text{mL}$  of CB biochar over time; (b) *L. plantarum* growth with 0, 50, and 100  $\mu\text{L}/\text{mL}$  of CB biochar over time. Different superscript letters indicate significant differences at  $p < 0.05$  among different concentrations within the same time point.

#### 4. Discussion

In this study, a mixture of woodchips and chestnut shells, which are an agricultural byproduct of chestnut production, was used to produce biochar through gasification in a Femto Gasifier system, in line with circular economy practices. The biochar was produced at temperatures exceeding  $500\text{ }^{\circ}\text{C}$ , which is considered suitable for animal feed. At these high temperatures, biochar retains beneficial volatile compounds while reducing harmful substances, such as polycyclic aromatic hydrocarbons (PAHs), which are more prevalent in biochar produced at lower temperatures [26].

Scanning electron microscopy (SEM) analysis of the chestnut biochar revealed a highly porous structure with fragments formed by fibers, vessels, parenchyma, and integument tissues. The presence of these tissues is coherent with the starting material used to produce biochar, such as wood and chestnut agro-residues (cupules, pericarps, and seeds). Fibers and vessels lignify the cell walls, which form the border of large channels and provide a substantial surface area for the exchange of chemicals, salts, ions, and metals. In addition, large parenchymatic cells, which lack proximal cell walls, increase the binding capacity of biochar.

Lignin is a complex organic polymer found in the cell walls of specific tissues, particularly in woody tissues and chestnut cupules/pericarps. Lignin-rich materials typically yield biochar with complex stable porous structures and higher pyrolysis temperatures further increase the porosity by removing volatile compounds and promoting the formation of a stable carbon matrix [27,28]. In chestnut biochar, the larger area of vessels and fibers lumen and parenchyma broken cells provide a higher absorption capacity for both binding organic molecules and bacterial colonization. In general, the porosity depends on the feedstock and production temperature. Biochar produced at temperatures greater than  $500\text{ }^{\circ}\text{C}$  also has a high porosity and a large surface area, which increase its ability to adsorb toxins and gases such as ammonia in the digestive system [29].

The chestnut biochar produced was alkaline, with a pH above 10, which is consistent with previous studies showing that biochar produced at temperatures exceeding  $500\text{ }^{\circ}\text{C}$  tends to be alkaline, while lower production temperatures yield more acidic biochar [27]. The alkalinity of biochar is influenced by the presence of salts, such as potassium, calcium carbonates, and chlorides. The chemical composition of biochar from chestnut agro-residues was characterized by a high ash content ( $25.00 \pm 0.25\%$ ), reflecting the significant presence of minerals, including potassium, sodium, magnesium, and calcium. Higher pyrolysis temperatures generally lead to increased ash content as organic matter decomposes, preserving the mineral content.

Heavy metal analysis of the chestnut biochar showed levels below the threshold set for use as a feed ingredient (Dir. 2002/32/EC), thus highlighting that the biochar is safe and of good quality for animal nutrition. Metabolomic analysis of the water extract revealed the presence of functional compounds, such as succinic acid, methyl coumarins, and small polyphenols. Succinic acid, which is an organic compound, is known for its strong antioxidant properties, as it acts as a metal scavenger and promotes the degradation of hydroperoxides without forming free radicals [30]. Coumarins, a class of organic compounds found in various plants, were also detected in the biochar. They are known for their diverse biological activities, including antimicrobial and anti-inflammatory properties. Specific derivatives, such as methylcoumarins, hydroxycoumarins, and methoxycoumarins, exhibit varying biological effects based on the addition of methyl (-CH<sub>3</sub>), hydroxyl (-OH), and methoxy (-OCH<sub>3</sub>) groups, respectively. Methylation enhances antimicrobial and anti-inflammatory properties, while hydroxyl and methoxy groups contribute to antioxidant activity.

Chestnut is also a rich source of bioactive polyphenols, including gallic acid, ellagic acid, quercetin, and catechins, which offer numerous health benefits [31]. However, these polyphenols are thermally unstable and degrade into smaller molecules during pyrolysis at temperatures above 500 °C. The degradation of plant cells during pyrolysis releases metabolites such as hydroxybenzoic acids, which are known for their antibacterial and antifungal properties. Hydroxybenzoic acid has been shown to disrupt bacterial cell membranes and inhibit essential microbial enzymes, leading to cell death [32]. It also interferes with fungal cell wall synthesis and provides antioxidant and anti-inflammatory effects [33]. The antioxidant potential of the biochar water extract is supported by Lameirão et al. (2020) [34], who reported the antioxidant activity of chestnut shell extract in water ranging from 50.5 to 88.00 µg/mL of Trolox equivalent (TE). This finding aligns with the antioxidant compounds found in the chestnut biochar, further confirming its potential for various applications, including animal feed.

The extract of chestnut biochar exhibited significant inhibitory activities against *E. coli*, particularly strains F4+ and F18+, which are key pathogens in enterotoxigenic infections in pigs. These infections can lead to severe health issues, especially in young animals. The ability of the biochar extract to inhibit bacterial growth suggests its potential for improving animal health by reducing pathogenic bacteria and limiting their replication in feed. Understanding the molecular mechanisms by which biochar extract interferes with *E. coli* growth is essential for optimizing its efficacy and developing targeted applications.

One important area of focus is the effect of the biochar extract on gene expression in *E. coli*, particularly genes involved in quorum sensing (QS), which regulates bacterial communication and biofilm formation. The formation of *E. coli* biofilms is controlled by a complex network of genes and metabolic pathways, which enable bacteria to coordinate their activities based on cell density [35,36]. Among these genes, the FliA gene encodes Sigma 28 (σ<sub>28</sub>), which plays a key role in regulating the expression of genes involved in flagellar biosynthesis and motility, including the production of flagellin (FliC) [37,38]. Additionally, sigma factors σ<sub>28</sub> and σ<sub>70</sub> regulate the expression of the MotA gene, which is crucial for the assembly and function of the bacterial flagellar motor.

Another key gene, FtsE, is part of the bacterial cell division machinery. It encodes a membrane protein that, together with FtsX, forms the FtsEX complex, which is essential for regulating the early stages of cell division and septum formation [39]. Disruption of FtsE expression can lead to defects in cell division, cell morphology, and viability, as well as increased susceptibility to antibiotics. The HflX gene encodes a GTP-binding protein involved in ribosome assembly, protein synthesis, and stress response mechanisms [39–41]. Down-regulation of HflX affects bacterial adaptation to environmental stress, including ribosome

biogenesis and cell division. Research has shown that FliA downregulation is associated with incomplete flagellar synthesis, reduced motility, and impaired chemotaxis [42], while disruption of FtsE leads to defects in cell division and morphology [43]. Similarly, loss of HflX function compromises the ability of bacteria to form stress granules, which are protective structures that help cells survive under stressful conditions [44]. It is likely that components of the chestnut biochar extract, particularly hydroxybenzoic acid, interfere with these bacterial processes. Hydroxybenzoic acid and its derivatives have demonstrated a quorum-sensing inhibitory activity. For example, Srivastava et al. (2020) [45] synthesized derivatives such as 3,4,5-trihydroxybenzoic acid methyl ester, which inhibited biofilm formation and communication between cells in *Chromobacterium violaceum*. Similarly, Zhou et al. (2022) [46] showed that 4-hydroxycinnamic acid, a hydroxybenzoic acid derivative, inhibited quorum sensing in *Agrobacterium tumefaciens*, reducing biofilm formation and pathogenicity.

In addition to its effects on pathogenic bacteria, the biochar extract was tested on two probiotic strains, *L. plantarum* and *L. reuteri*. Preliminary results suggest that at low concentrations, biochar extract may have a prebiotic effect, particularly on *L. plantarum*. The interactions between biochar and probiotics appear to depend on the unique metabolic pathways and genetic characteristics of each strain, as observed by Fan Yang et al. (2019) [47], who confirmed that the effects of biochar on bacterial growth are strain-dependent. Further research into the use of biochar as a feed additive could improve gut health in livestock by supporting beneficial probiotic populations, increasing nutrient absorption, and reducing disease incidence. The differing responses of *L. plantarum* and *L. reuteri* to biochar highlight the importance of understanding strain-specific interactions in optimizing the role of biochar as a functional ingredient for promoting gut health in animals.

The translation of in vitro data to in vivo doses is challenging, largely due to the inherent complexity of biological systems. A review of the literature revealed that biochar can be included in the feed in different concentrations, ranging from 0.3% to 6%. However, the reported outcomes are inconsistent, potentially due to the influence of dose-dependent effects [48]. A high inclusion percentage can have a negative effect on digestibility due to the adsorbent nature of the materials. It is therefore hypothesized that an inclusion percentage of less than 2% (percentage of additive included) is reasonable.

## 5. Conclusions

This study has focused on chestnut-derived biochar, highlighting its functional properties. Biochar positively promotes the growth of beneficial bacteria and inhibits the growth of pathogenic bacteria such as *Escherichia coli*. The bioactive compounds of chestnut biochar were demonstrated to possess antioxidant and antimicrobial activities, which are attributable to their capacity to interfere with quorum sensing. These results support the potential use of biochar as a functional additive in animal feed. This could provide significant benefits for animal health and improve ecosystem resilience and thus benefit both human and environmental health in alignment with the One Health perspective. This study highlights the importance of assessing specific biochar types, such as chestnut-derived biochar, to better understand their unique functional properties. In the context of a circular economy, which aims to minimize waste and maximize resource use, biochar production plays a crucial role by converting waste into a valuable product in alignment with the goals of sustainable livestock farming.

**Supplementary Materials:** The following supporting information can be downloaded at <https://www.mdpi.com/article/10.3390/app15031084/s1>, Figure S1: Representation of chromatograms of bioactive molecules detected by metabolomic analysis by QTOF HPLC MS-MS.

**Author Contributions:** Conceptualization, S.R., A.M., C.C. and L.R.; methodology, S.R., S.F., S.P. and N.M.; software, M.C.T. and N.M.; investigation, S.R., S.F., M.C.T., S.R.P., M.G. (Martina Ghidoli) and E.O.; resources, L.R. and S.P.; data curation, S.R., S.F., M.C.T., S.R.P., E.O. and A.M. writing—original draft preparation, S.R., S.F., M.P. and A.M.; writing—review and editing, S.F., S.R., L.R., A.M. and E.O.; visualization, S.R., M.G. (Marianna Guagliano), C.C. and M.P.; supervision, L.R., S.P. and A.M. All authors have read and agreed to the published version of the manuscript.

**Funding:** This research received no external funding.

**Institutional Review Board Statement:** Not applicable.

**Informed Consent Statement:** Not applicable.

**Data Availability Statement:** The authors confirm that the data supporting the findings of this study are available within the article [and/or] its Supplementary Materials.

**Conflicts of Interest:** M.C.T. was employed by Biotecnologie B.T. Srl. No commercial manufacturing products of Biotecnologie B.T. Srl. were used in this study. The remaining authors declare that the research was conducted in the absence of any commercial or financial relationships that could be construed as a potential conflict of interest.

## References

- Xiao, X.; Chen, B.; Chen, Z.; Zhu, L.; Schnoor, J.L. Insight into Multiple and Multilevel Structures of Biochars and Their Potential Environmental Applications: A Critical Review. *Environ. Sci. Technol.* **2018**, *52*, 5027–5047. [[CrossRef](#)]
- Giller, K.E.; Delaune, T.; Silva, J.V.; Descheemaeker, K.; van de Ven, G.; Schut, A.G.T.; van Wijk, M.; Hammond, J.; Hochman, Z.; Taulya, G.; et al. The Future of Farming: Who Will Produce Our Food? *Food Secur.* **2021**, *13*, 1073–1099. [[CrossRef](#)]
- FAO. *World Livestock: Transforming the Livestock Sector through the Sustainable Development Goals*; FAO: Rome, Italy, 2019; ISBN 978-92-5-130883-7.
- Ejileugha, C. Biochar Can Mitigate Co-Selection and Control Antibiotic Resistant Genes (ARGs) in Compost and Soil. *Heliyon* **2022**, *8*, e09543. [[CrossRef](#)] [[PubMed](#)]
- He, X.; Xiong, J.; Yang, Z.; Han, L.; Huang, G.Q. Exploring the Impact of Biochar on Antibiotics and Antibiotics Resistance Genes in Pig Manure Aerobic Composting Through Untargeted Metabolomics and Metagenomics. *Bioresour. Technol.* **2022**, *352*, 127118. [[CrossRef](#)] [[PubMed](#)]
- Kurniawan, T.A.; Othman, M.H.D.; Liang, X.; Goh, H.H.; Gikas, P.; Chong, K.-K.; Chew, K.W. Challenges and Opportunities for Biochar to Promote Circular Economy and Carbon Neutrality. *J. Environ. Manag.* **2023**, *332*, 117429. [[CrossRef](#)]
- Singh, E.; Mishra, R.; Kumar, A.; Shukla, S.K.; Lo, S.-L.; Kumar, S. Circular Economy-Based Environmental Management Using Biochar: Driving towards Sustainability. *Process Saf. Environ. Prot.* **2022**, *163*, 585–600. [[CrossRef](#)]
- Jindo, K.; Mizumoto, H.; Sawada, Y.; Sanchez-Monedero, M.A.; Sonoki, T. Physical and Chemical Characterization of Biochars Derived from Different Agricultural Residues. *Biogeosciences* **2014**, *11*, 6613–6621. [[CrossRef](#)]
- Ferraro, G.; Pecori, G.; Rosi, L.; Bettucci, L.; Fratini, E.; Casini, D.; Rizzo, A.M.; Chiaramonti, D. Biochar from Lab-Scale Pyrolysis: Influence of Feedstock and Operational Temperature. *Biomass Convers. Biorefinery* **2024**, *14*, 5901–5911. [[CrossRef](#)]
- Xie, Y.; Wang, L.; Li, H.; Westholm, L.J.; Carvalho, L.; Thorin, E.; Yu, Z.; Yu, X.; Skreiberg, Ø. A Critical Review on Production, Modification and Utilization of Biochar. *J. Anal. Appl. Pyrolysis* **2022**, *161*, 105405. [[CrossRef](#)]
- Gezae Daful, A.; Chandraratne, M.R.; Lorida, M. Recent Perspectives in Biochar Production, Characterization and Applications. In *Recent Perspectives in Pyrolysis Research*; IntechOpen: London, UK, 2022.
- Freitas, T.R.; Santos, J.A.; Silva, A.P.; Fraga, H. Influence of Climate Change on Chestnut Trees: A Review. *Plants* **2021**, *10*, 1463. [[CrossRef](#)]
- Szczurek, A. Perspectives on Tannins. *Biomolecules* **2021**, *11*, 442. [[CrossRef](#)] [[PubMed](#)]
- Basu, P. *Biomass Gasification and Pyrolysis: Practical Design and Theory*; Academic Press: Cambridge, MA, USA, 2010.
- Puig-Arnavat, M.; Bruno, J.C.; Coronas, A. Review and analysis of biomass gasification models. *Renew. Sustain. Energy Rev.* **2010**, *14*, 2841–2851. [[CrossRef](#)]
- Babu, B.V.; Sheth, P.N. Modeling and simulation of reduction zone of downdraft biomass gasifier: Effect of char reactivity factor. *Energy Convers. Manag.* **2006**, *47*, 2602–2611. [[CrossRef](#)]
- Latimer, J.W., Jr. (Ed.) *Official Method of Analysis of AOAC*, 22nd ed.; AOAC International: San Diego, CA, USA, 2023.
- Lou, Y.; Joseph, S.; Li, L.; Graber, E.R.; Liu, X.; Pan, G. Water Extract from Straw Biochar Used for Plant Growth Promotion: An Initial Test. *Bioresources* **2015**, *11*, 249–266. [[CrossRef](#)]

19. Perez, M.; Lopez, I.D.; Lamuela-Raventos, R.M. The Chemistry Behind the Folin-Ciocalteu Method for the Estimation of (Poly)phenol Content in Food: Total Phenolic Intake in a Mediterranean Dietary Pattern. *J. Agric. Food Chem.* **2023**, *71*, 17543–17553. [[CrossRef](#)] [[PubMed](#)]
20. Ilyasov, I.R.; Beloborodov, V.L.; Selivanova, I.A.; Terekhov, R.P. ABTS/PP Decolorization Assay of Antioxidant Capacity Reaction Pathways. *Int. J. Mol. Sci.* **2020**, *21*, 1131. [[CrossRef](#)] [[PubMed](#)]
21. Rao, X.; Huang, X.; Zhou, Z.; Lin, X. An improvement of the  $2^{-\Delta\Delta CT}$  method for quantitative real-time polymerase chain reaction data analysis. *Biostat. Bioinform. Biomath.* **2013**, *3*, 71–85.
22. Sun, T.; Li, X.D.; Hong, J.; Liu, C.; Zhang, X.L.; Zheng, J.P.; Xu, Y.J.; Ou, Z.Y.; Zheng, J.L.; Yu, D.J. Inhibitory Effect of Two Traditional Chinese Medicine Monomers, Berberine and Matrine, on the Quorum Sensing System of Antimicrobial-Resistant *Escherichia coli*. *Front. Microbiol.* **2019**, *10*, 2584. [[CrossRef](#)]
23. Dell'Anno, M.; Callegari, M.L.; Reggi, S.; Caprarulo, V.; Giromini, C.; Spalletta, A.; Coranelli, S.; Sgoifo Rossi, C.A.; Rossi, L. Lactobacillus Plantarum and Lactobacillus Reuteri as Functional Feed Additives to Prevent Diarrhoea in Weaned Piglets. *Animals* **2021**, *11*, 1766. [[CrossRef](#)]
24. Dell'Anno, M.; Giromini, C.; Reggi, S.; Cavalleri, M.; Moscatelli, A.; Onelli, E.; Rebutti, R.; Sundaram, T.S.; Coranelli, S.; Spalletta, A.; et al. Evaluation of Adhesive Characteristics of *L. Plantarum* and *L. Reuteri* Isolated from Weaned Piglets. *Microorganisms* **2021**, *9*, 1587. [[CrossRef](#)]
25. Schoch, W.; Heller, I.; Schweingruber, F.H.; Kienast, F. *Wood Anatomy of Central European Species*; Swiss Federal Institute for Forest: Birmensdorf, Switzerland, 2004.
26. Devi, P.; Dalai, A.K. Occurrence, Distribution, and Toxicity Assessment of Polycyclic Aromatic Hydrocarbons in Biochar, Biocrude, and Biogas Obtained from Pyrolysis of Agricultural Residues. *Bioresour. Technol.* **2023**, *384*, 129293. [[CrossRef](#)]
27. Leng, L.; Xiong, Q.; Yang, L.; Li, H.; Zhou, Y.; Zhang, W.; Jiang, S.; Li, H.; Huang, H. An Overview on Engineering the Surface Area and Porosity of Biochar. *Sci. Total Environ.* **2021**, *763*, 144204. [[CrossRef](#)] [[PubMed](#)]
28. Grottola, C.M.; Giudicianni, P.; Stanzione, F.; Ragucci, R. Influence of Pyrolysis Temperature on Biochar Produced from Lignin-Rich Biorefinery Residue. *ChemEngineering* **2022**, *6*, 76. [[CrossRef](#)]
29. Hossain, M.K.; Strezov, V.; Chan, K.Y.; Ziolkowski, A.; Nelson, P.F. Influence of Pyrolysis Temperature on Production and Nutrient Properties of Wastewater Sludge Biochar. *J. Environ. Manag.* **2011**, *92*, 223–228. [[CrossRef](#)] [[PubMed](#)]
30. Bespyatykh, O.Y.; Kokorina, A.E.; Domsik, I.A. State of Antioxidant System of Furbearers after Injection of Succinic Acid. *Russ. Agric. Sci.* **2011**, *37*, 516–519. [[CrossRef](#)]
31. Barreira, J.C.M.; Ferreira, I.C.F.R.; Oliveira, M.B.P.P. Bioactive Compounds of Chestnut (*Castanea sativa* Mill.). In *Bioactive Compounds in Underutilized Fruits and Nuts. Reference Series in Phytochemistry*; Murthy, H., Bapat, V., Eds.; Springer: Cham, Switzerland, 2020. [[CrossRef](#)]
32. Campos, F.M.; Couto, J.A.; Figueiredo, A.R.; Tóth, I.V.; Rangel, A.O.S.S.; Hogg, T.A. Cell Membrane Damage Induced by Phenolic Acids on Wine Lactic Acid Bacteria. *Int. J. Food Microbiol.* **2009**, *135*, 144–151. [[CrossRef](#)]
33. Khan, S.A.; Chatterjee, S.S.; Kumar, V. Low Dose Aspirin like Analgesic and Anti-Inflammatory Activities of Mono-Hydroxybenzoic Acids in Stressed Rodents. *Life Sci.* **2016**, *148*, 53–62. [[CrossRef](#)]
34. Lameirão, F.; Pinto, D.; Vieira, E.F.; Peixoto, A.F.; Freire, C.; Sut, S.; Dall'Acqua, S.; Costa, P.; Delerue-Matos, C.; Rodrigues, F. Green-Sustainable Recovery of Phenolic and Antioxidant Compounds from Industrial Chestnut Shells Using Ultrasound-Assisted Extraction: Optimization and Evaluation of Biological Activities In Vitro. *Antioxidants* **2020**, *9*, 267. [[CrossRef](#)] [[PubMed](#)]
35. Rutherford, S.T.; Bassler, B.L. Bacterial Quorum Sensing: Its Role in Virulence and Possibilities for Its Control. *Cold Spring Harb. Perspect. Med.* **2012**, *2*, a012427. [[CrossRef](#)]
36. Sun, Y.; Kim, S.W. Intestinal Challenge with Enterotoxigenic *Escherichia coli* in Pigs, and Nutritional Intervention to Prevent Postweaning Diarrhea. *Anim. Nutr.* **2017**, *3*, 322–330. [[CrossRef](#)]
37. Clarke, M.B.; Sperandio, V. Transcriptional Regulation of *FliHDC* by QseBC and  $\sigma^{28}$  (FliA) in Enterohaemorrhagic *Escherichia coli*. *Mol. Microbiol.* **2005**, *57*, 1734–1749. [[CrossRef](#)] [[PubMed](#)]
38. Fitzgerald, D.M.; Bonocora, R.P.; Wade, J.T. Comprehensive Mapping of the *Escherichia coli* Flagellar Regulatory Network. *PLoS Genet.* **2014**, *10*, e1004649. [[CrossRef](#)] [[PubMed](#)]
39. Mallik, S.; Dodia, H.; Ghosh, A.; Srinivasan, R.; Good, L.; Raghav, S.K.; Beuria, T.K. FtsE, the Nucleotide Binding Domain of the ABC Transporter Homolog FtsEX, Regulates Septal PG Synthesis in *E. coli*. *Microbiol. Spectr.* **2023**, *11*, e02863-22. [[CrossRef](#)] [[PubMed](#)]
40. Shields, M.J.; Fischer, J.J.; Wieden, H.-J. Toward Understanding the Function of the Universally Conserved GTPase HflX from *Escherichia coli*: A Kinetic Approach. *Biochemistry* **2009**, *48*, 10793–10802. [[CrossRef](#)] [[PubMed](#)]
41. Dey, S.; Biswas, C.; Sengupta, J. The Universally Conserved GTPase HflX Is an RNA Helicase That Restores Heat-Damaged *Escherichia coli* Ribosomes. *J. Cell Biol.* **2018**, *217*, 2519–2529. [[CrossRef](#)]
42. Seely, S.M.; Gagnon, M.G. Mechanisms of Ribosome Recycling in Bacteria and Mitochondria: A Structural Perspective. *RNA Biol.* **2022**, *19*, 662–677. [[CrossRef](#)]

43. Rodríguez-Herva, J.J.; Duque, E.; Molina-Henares, M.A.; Navarro-Avilés, G.; Van Dillewijn, P.; De La Torre, J.; Molina-Henares, A.J.; La Campa, A.S.; Ran, F.A.; Segura, A.; et al. Physiological and Transcriptomic Characterization of a *FliA* Mutant of *Pseudomonas putida* KT2440. *Environ. Microbiol. Rep.* **2010**, *2*, 373–380. [[CrossRef](#)] [[PubMed](#)]
44. Souquere, S.; Mollet, S.; Kress, M.; Dautry, F.; Pierron, G.; Weil, D. Unravelling the Ultrastructure of Stress Granules and Associated P-Bodies in Human Cells. *J. Cell Sci.* **2009**, *122*, 3619–3626. [[CrossRef](#)]
45. Srivastava, N.; Tiwari, S.; Bhandari, K.; Biswal, A.K.; Rawat, A.K.S. Novel Derivatives of Plant Monomeric Phenolics: Act as Inhibitors of Bacterial Cell-to-Cell Communication. *Microb. Pathog.* **2020**, *141*, 103856. [[CrossRef](#)] [[PubMed](#)]
46. Zhou, J.-W.; Ji, P.-C.; Jiang, H.; Tan, X.-J.; Jia, A.-Q. Quorum Sensing Inhibition and Metabolic Intervention of 4-Hydroxycinnamic Acid Against *Agrobacterium tumefaciens*. *Front. Microbiol.* **2022**, *13*, 830632. [[CrossRef](#)] [[PubMed](#)]
47. Yang, F.; Zhou, Y.; Liu, W.; Tang, W.; Meng, J.; Chen, W.; Li, X. Strain-Specific Effects of Biochar and Its Water-Soluble Compounds on Bacterial Growth. *Appl. Sci.* **2019**, *9*, 3209. [[CrossRef](#)]
48. Chu, G.M.; Kim, J.H.; Kim, H.Y.; Ha, J.H.; Jung, M.S.; Song, Y.; Cho, J.H.; Lee, S.J.; Ibrahim, R.I.H.; Lee, S.S.; et al. Effects of bamboo charcoal on the growth performance, blood characteristics and noxious gas emission in fattening pigs. *J. Appl. Anim. Res.* **2013**, *41*, 48–55. [[CrossRef](#)]

**Disclaimer/Publisher’s Note:** The statements, opinions and data contained in all publications are solely those of the individual author(s) and contributor(s) and not of MDPI and/or the editor(s). MDPI and/or the editor(s) disclaim responsibility for any injury to people or property resulting from any ideas, methods, instructions or products referred to in the content.